

1 Experimental study and numerical reproduction of self-weight 2 consolidation behavior of thickened tailings

3

4 Michaël Demers Bonin¹; Mathieu Nuth, Ph.D.²; Alexandre Cabral, Ph.D., P.Eng.^{2,*}; Anne-Marie
5 Dagenais, Ph.D., P.Eng.³

6

7 ABSTRACT

8 Thickened tailings, defined as mineral wastes that behave as a non-Newtonian fluid, show a small yield stress
9 and release a small amount of water following deposition. Thickening has become an increasingly used option in
10 tailings management. This paper presents a detailed examination of gold mine thickened tailings undergoing self-
11 weight consolidation, which is an important mechanism affecting soft soils immediately after deposition. Self-
12 weight consolidation was evaluated using a column equipped with water pressure transmitters whereas a slurry
13 consolidometer was employed to obtain the compressibility relationship under low vertical effective stresses. The
14 piecewise-linear model CS2 was used to model the experimental self-weight consolidation test. This model
15 proved very accurate in reproducing the observed behavior. The test results as well as the model results also
16 confirmed the absence of sedimentation in the thickened tailings, which is in agreement with values reported in
17 the literature related to similar materials.

18

19 INTRODUCTION

20

21 The technology of thickened tailings (TT) has gained the attention of the mining industry in the last thirty years,
22 as several mines adopted a TT approach to tailings management (Williams and Ennis 1996; McPhail et al. 2004;
23 Oxenford and Lord 2006; Barbour et al. 1993). Many advantages have been reported since the development of
24 this technology by Robinsky in 1973 (Robinsky 1975), including a reduced amount of water released following
25 deposition, as well as the possibility of stacking tailings with a greater beach angle than non-thickened tailings
26 (Robinsky 1999). However, Fourie (2012) questions whether or not the attributed benefits to TT have in fact been
27 realized. Thickened or not, a key consideration in tailings management is the storage capacity of tailings disposal
28 areas (TDA). This aspect is in fact largely affected by how tailings settle. Understanding the settlement behavior
29 of thickened tailings is paramount to furthering the use of TT technology.

30

31 In this context, extensive research has been undertaken in the recent past to define the most important
32 mechanisms causing settlement in soft deposits such as marine sediments, dredging residues and mine tailings.
33 Mikasa (1965), followed by Gibson et al. (1967), published a theory on large strain consolidation of soft clays.
34 Further studies were published on the issue of large strain consolidation of soft deposits; Imai (1980; 1981),

¹ Graduate student, Dept. of Civil Engineering, Université de Sherbrooke, 2500, boul. de l'Université,
Sherbrooke, QC, CANADA J1K 2R1

² Professor, Dept. of Civil Engineering, Université de Sherbrooke, 2500, boul. de l'Université,
Sherbrooke, QC, CANADA J1K 2R1

³ Golder Associés Ltée., 1001 boul. de Maisonneuve O., 7th Floor, Montreal, QC, CANADA H3A 3C8

*Corresponding author: alexandre.cabral@usherbrooke.ca

35 Been and Sills (1981), Schiffman et al. (1988) and Tan et al. (1990) made fundamental contributions by including
36 flocculation, sedimentation and self-weight consolidation. These physical mechanisms were found to be the first
37 processes influencing settlement of soft deposits after deposition.

38

39 The removal of process water affects the settlement processes immediately after deposition, insofar as it can
40 inhibit (or at least reduce) the flocculation and sedimentation phases that precede or overlap self-weight
41 consolidation. In other words, depending on the solids content, self-weight consolidation may be the sole
42 mechanism responsible for thickened tailings settlement and dissipation of excess pore water pressure (EPWP)
43 after deposition.

44

45 This paper analyzed self-weight consolidation of TT samples in a unique way by combining slurry deposition in
46 settling columns, consolidation tests in a consolidometer and the use of a numerical model to reproduce the
47 observed results. The evolution of pore water pressure values during the tests performed in the settling columns
48 and the accuracy with which these results were reproduced by the piecewise-linear model CS2 have made it
49 possible to clearly document an important element about the phenomena of self-weight consolidation. This
50 element relates to the fact that the settlement of the tailings-water interface generated by the region undergoing
51 self-weight consolidation affects excess pore water pressures in the region immediately above, which itself is
52 about to undergo self-weight consolidation.

53

54

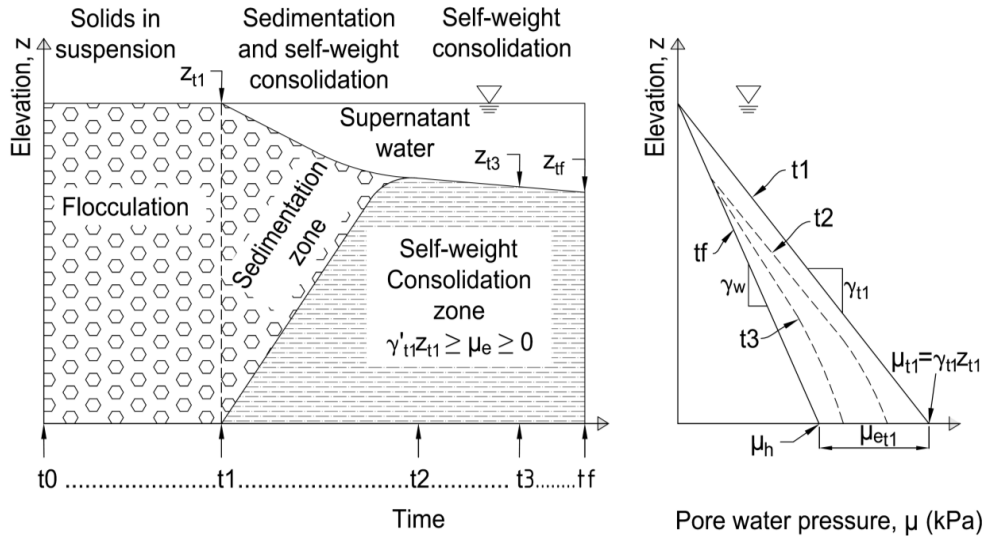
55

56 **REVIEW OF SELF-WEIGHT CONSOLIDATION AND ITS MODELING**

57

58 Different behaviors may be observed in soft deposits or hydraulic fills, such as flocculation, sedimentation and
59 self-weight consolidation (Fig.1). Initially, the particles are in suspension in a dense fluid medium. Self-weight
60 consolidation begins as soon as the solid particles build a skeleton whereby soil particles transmit their weight to
61 the bottom (following time t_1 in Fig.1) (Been and Sills 1981), while dissipation of EPWP (μ_e in Fig.1) occurs
62 simultaneously with settlement. The driving mechanism is the dissipation of EPWP, which is caused by the
63 buoyant unit weight of the soil particles. When self-weight consolidation starts, the effective stress builds up and
64 the slurry starts to behave as a soil. Self-weight consolidation is over when the soil stratum is in equilibrium under
65 its own weight (time t_f in Fig.1).

66



67
68 **Fig. 1.** Sedimentation and self-weight consolidation processes expressed in terms of the settlement-time
69 response (left) (adapted from Imai, 1981) and dissipation of pore water pressure with elevation when self-weight
70 consolidation dominates (right)

71
72 Settling columns are commonly used to evaluate self-weight consolidation of soft deposits. In column tests, the
73 initial void ratio is uniform. In addition, effective stress and self-weight consolidation start simultaneously. Alexis
74 et al. (2004) provide further details on settling column experiments, in which the transition from a settling
75 suspension regime (sedimentation) to a soil formation regime (self-weight consolidation) can be observed. Been
76 and Sills (1981) observed the development of effective stress together with structural density that seemed to
77 indicate the transition from a settling suspension to a soil formation. This transition was also described in terms of
78 critical water content (Imai 1980), of void ratio (Carrier III et al. 1983; Pane and Schiffman 1985; de Oliveira-Filho
79 and van Zyl 2006; Jeeravipoolvarn et al. 2009a; Azam 2011), or in terms of volumetric solid concentration (Li and
80 Williams 1995a; Burger and Concha 1998). Tan (1995) proposed that a significant increase in shear strength
81 marks the transition from a suspension to a soil. In silt-like materials, Oliveira-Filho and van Zyl (2006) proposed
82 that sedimentation starts to be negligible at a void ratio of 2.20 while Bartholomeeusen et al. (2002) studied the
83 self-weight consolidation of silt-like river sediment at initial void ratios between 2.09 and 4.48.

84
85 Several authors attempted to use numerical codes to predict the results of experimental self-weight consolidation
86 tests performed on various types of soils, dredging residues and mine tailings. Been and Sills (1981) used an
87 analytical solution to the Gibson's finite strain consolidation theory. McVay et al. (1986), Hawlader et al. (2008)
88 and Jeeravipoolvarn et al.(2009b) used a numerical solution of the Gibson's equation. Berilgen et al. (2006)
89 preferred to use a piecewise-linear model. Townsend and McVay (1990) showed that a numerical solution of the
90 finite strain theory and a piecewise-linear model yielded similar predictions of self-weight consolidation. In turn,
91 the use of analytical solutions to the finite-strain consolidation theory appears too limiting to predict consolidation
92 behavior of soft deposits because of restrictive assumptions that simplify the solution. Nonetheless, they are
93 convenient to validate numerical solutions of finite-strain consolidation of special cases as demonstrated by
94 Morris (2002) and Xie and Leo (2004).

96 The selection of a characteristic $e - \sigma'_v$ relationship is a key factor in modeling self-weight consolidation
97 settlement of soft deposits in settling columns. A major difficulty is measuring low effective stresses occurring
98 during the self-weight consolidation. Been and Sills (1981), Alexis (2004) and Pedroni (2011) overcame this
99 difficulty by measuring the evolution of density using accurate non-destructive apparatuses (X-ray and γ -ray).
100 With density and pore water it is possible to evaluate the vertical effective stress within the settling column at any
101 time, thus estimate a $e - \sigma'_v$ relationship (Been and Sills 1981; Sills 1998). Toorman (1999) suggested
102 nonetheless that the measurements of the lower effective stresses, especially in the top 10 cm, may not be
103 reliable due to the imprecision of the density and the pore water pressure measurements.

104

105 **MATERIALS AND METHODS**

106

107 ***Materials***

108

109 The tailings samples were taken from a gold mine tailings facility (location to remain undisclosed). At their arrival
110 at the Soil Mechanics Laboratory of the Université de Sherbrooke, the tailings within the pails had settled, as
111 evidenced by the presence of supernatant water. The average gravimetric water content (w) of the settled
112 material was approximately 34.7%. The gravimetric water content was about 50.7% after being homogenized
113 with the supernatant water, corresponding to a tailings solids content of 66.4% (mass of dry solids divided by the
114 total mass of solids). For this study, the material was brought to a solids content of 68% ($e_o=1.3$, for a degree of
115 saturation of 100% and specific gravity, G_s of 2.76) by drying and re-homogenizing with distilled water. This is
116 generally considered to be in the range of reported solids content (50% to 70%) for hard rock mine TT (McPhail
117 et al. 2004; Oxenford and Lord 2006; Fourie 2012; Bussière 2007). As confirmed by assessment tests (results
118 not presented herein), the use of distilled water instead of process water did not lead to any significant variation
119 in the EPWP dissipation during self-weight consolidation. The mine tailings studied in this project correspond to
120 a silt-sized material of low plasticity, a classification often reported for gold mine tailings (de Oliveira-Filho and
121 van Zyl 2006; Bussière 2007). Table 1 summarizes the geotechnical characteristics of the studied tailings. In
122 addition, hydraulic conductivities of 4.20×10^{-8} m/s, 4.99×10^{-8} m/s, 5.66×10^{-8} m/s and 6.22×10^{-8} m/s for void ratios
123 of 0.61, 0.65, 0.67 and 0.69, respectively, were obtained from falling head permeability tests performed in the
124 oedometer cell. The oedometric consolidation tests (whose results are presented in Fig.6 and discussed later)
125 started at void ratios between 0.88 and 0.89 and were performed according to ASTM D2435-11 in a 101.6-mm
126 interior diameter cell. Compression indexes (C_c) were comprised between 0.052 and 0.070 and the
127 recompression index (C_r) was 0.011. Compression indexes between 0.050 to 0.150, for initial void ratios between
128 0.5 to 1.0, have often been reported (e.g. McPhail et al. 2004; Mittal and Morgenstern 1976; Blight and Steffen
129 1979; Aubertin et al. 1996; Yunxin (Jason) and Segó 2001; Crowder 2004; Fahey et al. 2010)

130

131

132

133

134

Table 1. Characteristics of the studied gold mine tailings

Characteristics	ASTM Standard	Gold mine tailings
Specific gravity, G_s	ASTM D854-10	2.76
Liquid limit, W_L (%)	ASTM D4318-10	29 ^a
Plastic limit, W_P (%)		25 ^b
Plasticity index, I_P (%)		4
Sand >75 μ m (%)		8
Silt (%)		81
Clay-sized particles <2 μ m (%)		11
D_{10} (mm)	ASTM D422-63	0.0018
D_{60} (mm)		0.021
Uniformity coefficient, C_u		12
USCS classification		ML

^a Determined with the Swedish cone method

^b Based on one (1) sample

136

137

138

139

140 **Laboratory equipment and experimental procedure**

141

142 *Settling column*

143

144 Self-weight consolidation experiments were conducted in a settling column represented in Fig. 2. The settling
 145 column is made of clear acrylic with an internal diameter of 101.6 mm. Total pore water pressure was monitored
 146 at three elevations (bottom, 0.1 m and 0.2 m) via pressure transmitters (BD|Sensors LMP 331, range of 0 to 10
 147 kPa, accuracy of ± 0.01 kPa) screwed to the column wall. The saturation chambers helped to establish saturation
 148 in the lines between the pressure transmitters and the embedded porous stones. The output signal from the
 149 pressure transmitters was monitored with a measuring instrument (Handyscope HS4 by TiePie engineering)
 150 coupled with the software *Tie-Pie Multi Channel* (TiePie engineering). The transmitters are excited by a 20 V
 151 external power supply. It was assumed that the column wall friction was negligible due to the use of a column
 152 diameter greater than 100 mm (Elder 1985; Migniot 1989; Sills 1997). Since the phenomenon of self-weight
 153 consolidation was primarily studied in terms of EPWP dissipation, no actual direct density measurement was
 154 performed in this study. As detailed later, the void ratio/vertical effective stress and the hydraulic conductivity/void
 155 ratio relationships were not obtained directly from the settling column experiments.

156

157 Once the porous stones had been saturated, the column was emptied and each transducer reading was set to
 158 zero on the data logging system. Tailings were then poured to a height of 300 mm, and the sample was
 159 homogenized to reach a uniform void ratio distribution. Total pore water pressure (μ) data started being recorded
 160 after the mixer was removed from the sample. Water expelled from tailings during self-weight consolidation
 161 formed a supernatant layer in the column. After completion of self-weight consolidation (i.e. once EPWP had
 162 been completely dissipated), the tailings height was recorded, the supernatant water was weighted and samples
 163 were taken at the top and bottom of the column for water content determination. Void ratios were calculated from
 164 water content measurements, and by assuming complete saturation. EPWP (μ_e) was calculated by subtracting
 165 the hydrostatic pressure (μ_h) from the total pore water pressure.

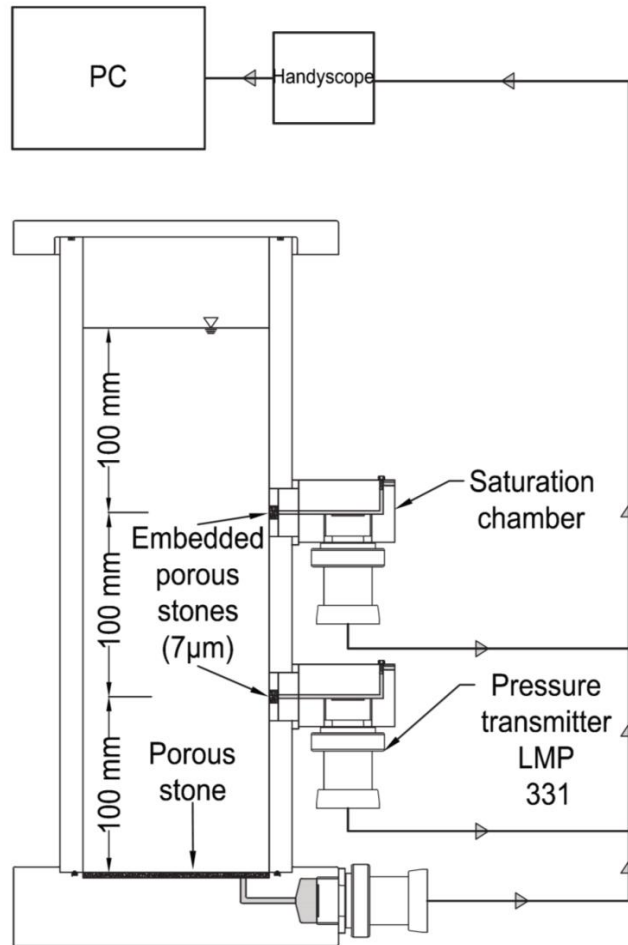


Fig. 2. 300-mm-high settling column

166

167

168

169 *Consolidometer*

170

171 The consolidometer shown in Fig.3 was used for self-weight and primary consolidation. The apparatus is similar
 172 to slurry consolidometers used elsewhere to obtain a $e - \sigma'_v$ relationships for samples submitted to large strains
 173 (Yunxin (Jason) and Seg0 2001; Bromwell and Carrier 1979; Wong et al. 2008). It consists of a 100-mm-high
 174 acrylic column equipped with a water pressure transmitter installed at the base. A counterweight-swivel system
 175 was developed to support the mass of the loading piston. Since the latter does not apply any additional stress to
 176 the sample, initial low stress increments can be applied.

177

178 For the self-weight consolidation phase, the testing procedure is the same as in the 300-mm-high settling
 179 column. Once the sample had consolidated under its own weight, the height of the sample and the thickness of
 180 supernatant water were recorded. The loading piston was then gently lowered until it came into contact with the
 181 tailings surface. Loadings corresponding to stresses ($\Delta\sigma$) of 0.06, 0.12, 0.3, 0.61, 1.1, 2.2, 4.4 and 8.8 kPa were
 182 applied to the tailings surface. The strain was recorded before applying a new load. The dry mass of solids was
 183 measured at the end of the experiment. An average void ratio throughout the column was calculated using the
 184 height of the sample and the height of solids $(H - H_s)/H_s$. The vertical effective stress was considered to be

185 equal to the load increment stress ($\Delta\sigma = \sigma'$) since the self-weight stress of the sample and the hydrostatic
186 pressure were neglected as is often reported in the technical literature (e.g. Bromwell and Carrier 1979;
187 Yunxin(Jason) and Seg0 2001; Wong et al. 2008).

188

189 Demers Bonin et al. (2013) reported the dissipation of EPWP with time during self-weight consolidation of TT
190 samples ($e_o = 1.3$) with initial heights of 100 mm and 300 mm. These results showed that the trend of dissipation
191 of EPWP measured at the bottom of samples of both heights was nearly the same. Subsequently, the $e - \sigma'_v$
192 relationship obtained from the consolidometer is assumed to represent the compressibility behavior of the 300-
193 mm-high TT samples at low effective stresses. Complementary data were obtained from standard consolidation
194 tests carried out with a 4 inch oedometer cell placed in a conventional oedometric apparatus, using dead-weight
195 loading.

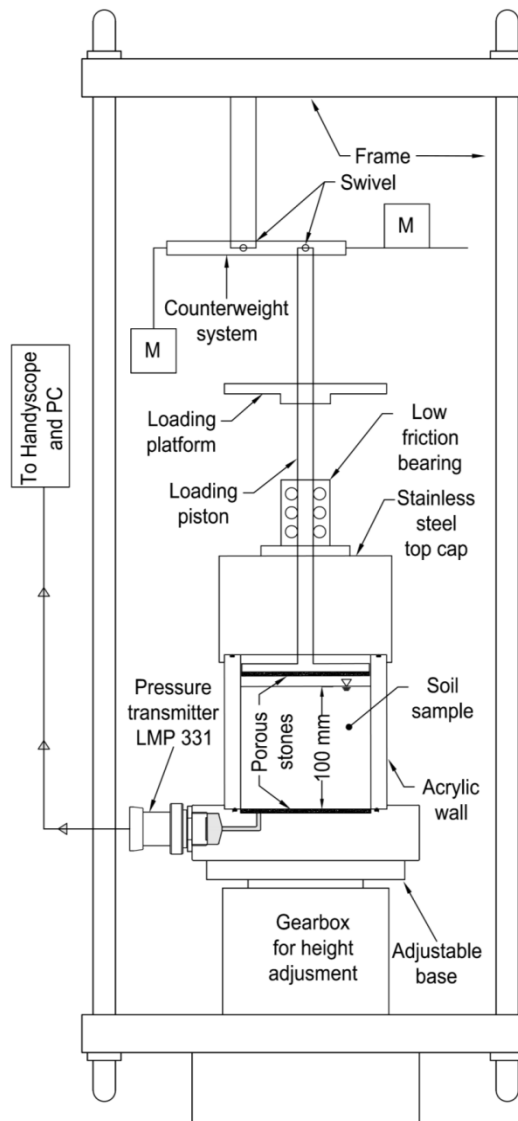


Fig. 3. Consolidometer setup

196

197

198

199 THE CS2 NUMERICAL MODEL

200

201 The CS2 numerical model (Fox and Berles 1997) was used to reproduce the behavior of the fine-grained tailings
202 during self-weight consolidation. CS2 was developed to predict large-strain consolidation and is based on a one-
203 dimensional piecewise-linear finite difference model. The initial geometry is discretized in vertical elements that
204 have constant properties during each time increment. The number of vertical elements (R_i) defined by the user
205 affects the accuracy of the results. CS2 accounts for large strain, self-weight effects, relative velocity of fluid and
206 solid phases and non-linearity of hydraulic conductivity and compressibility. The code was implemented in Matlab
207 and its capability was verified with the four verification problems presented by Fox and Berles (1997). The input
208 includes two constitutive relationships in the form of discrete point functions. One function represents
209 compressibility as an effective stress-dependent function and the other represents hydraulic conductivities as a
210 void ratio-dependent function. Additional inputs needed for a CS2 simulation are: specific gravity, water head at
211 bottom and at the top, the duration of the analysis and the initial effective stress associated with the initial void
212 ratio (e_o). CS2 does not account for sedimentation of solid particles (Fox 2000).

213

214 A third time step criterion was added to the code to ensure numerical stability. It was observed that self-weight
215 effects were responsible for high hydraulic gradients in the very beginning of the simulation near the bottom of
216 the column. By implementing the time step criteria provided by Fox (2000), the code ensures that the change in
217 element height for any time step is no greater than 0.5%. Moreover, the code was modified to consider a uniform
218 void ratio distribution in the beginning of self-weight consolidation. The user specifies the initial void ratio and
219 CS2 refers to the compressibility constitutive relationship to find the initial effective stress. In theory, the effective
220 stress equals zero in the beginning of self-weight consolidation but a value different from zero is required to run
221 CS2.

222

223 RESULTS AND DISCUSSION

224

225 *Self-weight consolidation: settling column*

226

227 From a total of 16 tests performed in the 300-mm-high settling column, 4 had the same initial conditions (see
228 Table 2). At the end of self-weight consolidation, there was a supernatant water layer at the top of the column,
229 resulting from an average vertical strain of 11.7% and an average increase in density ($\rho_f - \rho_o$) of 111 kg/m³. The
230 initial void ratios (e_o) were nearly equal for the four tests, while at the end of the self-weight consolidation, the
231 bottom of the column was denser. Final void ratio values ranged between 1.11 and 1.16 at the top (e_{ft}) and
232 between 1.00 and 1.01 at the bottom (e_{fb}). The greater density at the bottom of the column is caused by the
233 increasing weight of slurry with depth.

234

235 Fig. 4 presents the evolution of average dissipation of EPWP with time and the corresponding standard
236 deviations. The greatest standard deviations for the four tests are noticeable between 500 and 1100 min, i.e.
237 approximately halfway through the self-weight consolidation process. The intercepts with the y-axis in Fig. 4 are
238 2.24 kPa (at the bottom), 1.52 kPa (0.1 m above bottom) and 0.72 kPa (0.2 m above bottom). From the average
239 initial density (ρ_o) and the mean initial height (H_o), the theoretical intercepts with the y-axis are respectively, 2.29

240 kPa, 1.53 kPa and 0.76 kPa. Dissipation of EPWP at the base (0 m) began immediately after homogenization of
 241 the sample in the column, while dissipation of EPWP at 0.1 m and 0.2 was slower (dissipation curves are
 242 smoother). The results in Fig. 4 indicate that self-weight consolidation started at approximately 300 min at an
 243 elevation of 0.1 m above the bottom, and at 600 min at 0.2 m above the bottom. Before self-weight consolidation
 244 reached 0.1 m and then 0.2 m, there was still a slow decrease in EPWP. Apparently, this slow dissipation was
 245 caused by self-weight consolidation at the bottom. Indeed, the tailings-water interface moving down by self-
 246 weight consolidation generated a decrease in the height of solids, which, in turn, reduced the excess pore water
 247 pressure (μ_e) at 0.1 m and 0.2 m ($\mu_e = \gamma' H$). Theoretically, the part of the column undergoing self-weight
 248 consolidation causes a change in the void ratio distribution, while the part of the column that has not begun self-
 249 weight consolidation remains at its initial void ratio. Consequently, in the present case, the EPWP in the
 250 uppermost part that had not begun to consolidate was affected by the tailings-water interface settlement (H is
 251 decreasing), while the buoyant unit weight (γ') remained constant. Self-weight consolidation was complete after
 252 1440 minutes (24 hours) for all 4 tests.

253

254 **Table 2.** Summary of self-weight consolidation tests in the 300-mm-high settling column

255

Test #	H_0 (m)	Initial void ratio, e_0	ρ_0 (kg/m ³)	Mass of tailings deposited (g)	H_f (m)	Final void ratio (top), e_{ft}	Final void ratio (bottom), e_{fb}	ρ_f average (kg/m ³)	$\Delta\rho$ (kgm ³)	Mass of supernatant water on top (g)	Vertical strain (%)
6	0.302	1.28	1769.8	4330.4	0.266	1.12	1.00	1880.6	110.8	270.79	11.8
7	0.300	1.29	1787.8	4345.4	0.265	1.16	1.01	1897.6	109.8	264.48	11.5
14	0.301	1.28	1786.9	4357.6	0.267	1.13	1.01	1897.2	110.3	254.45	11.3
16	0.298	1.29	1772.2	4285.3	0.262	1.11	1.00	1886.9	114.7	281.06	12.2
avg	0.300	1.29	1779.2	4329.7	0.265	1.13	1.00	1890.6	111.4	267.7	11.7

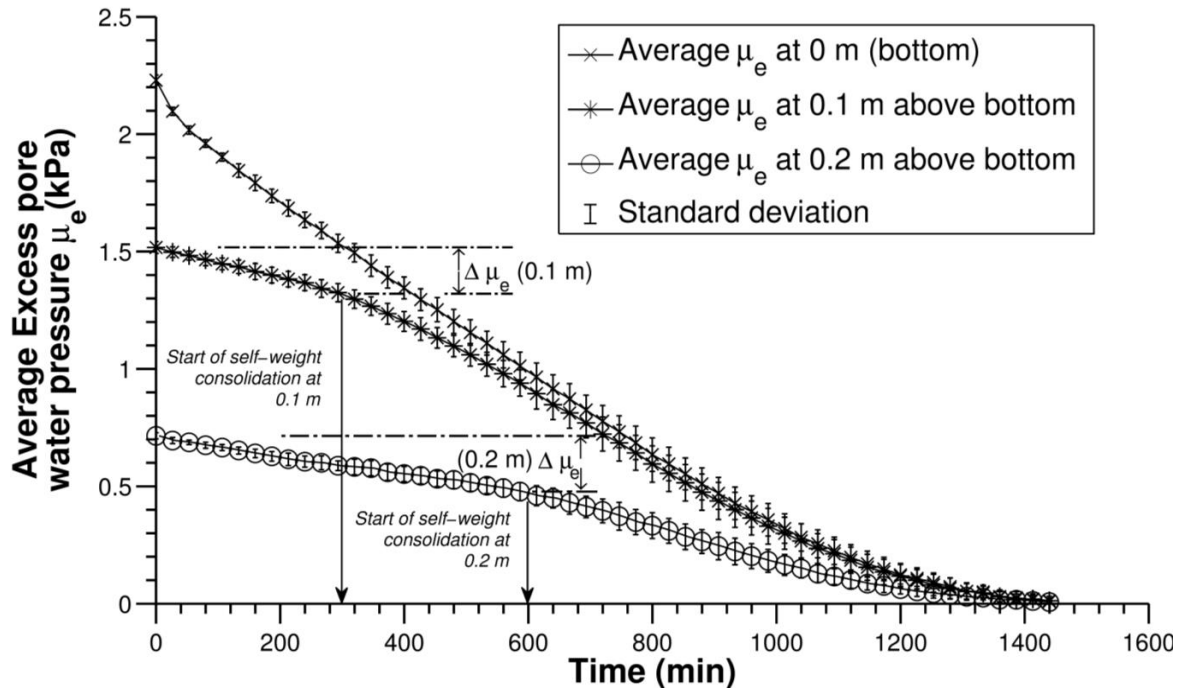
256

257 Variations above and below the average dissipation curves in Fig. 4 were possibly due to slight differences in
 258 initial experimental conditions, such as initial height or initial water content or slight variations in grain size or
 259 mineralogy. Those may have influenced dissipation of EPWP since they can affect the hydraulic conductivity or
 260 the specific gravity of the samples.

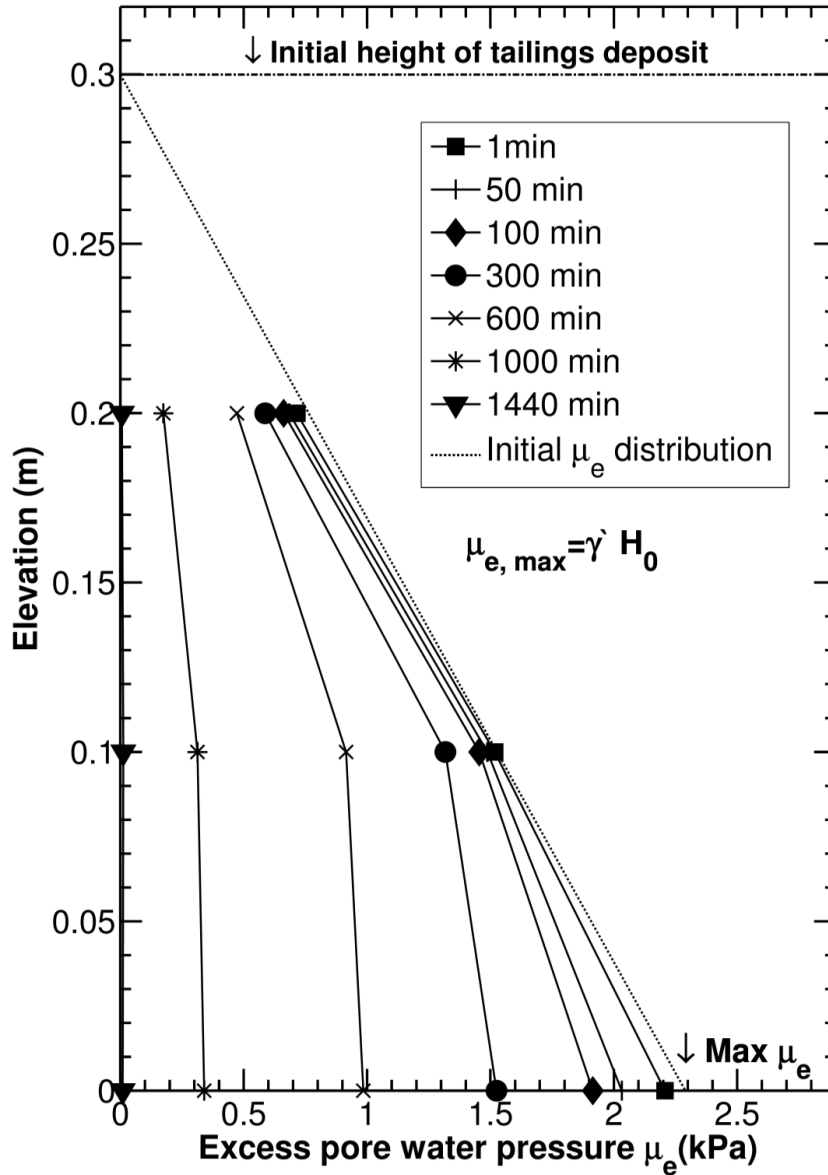
261

262 Fig. 5 presents the elevation versus average EPWP at the same elevations (bottom, 0.1 m and 0.2 m). The
 263 theoretical maximum EPWP developed in the beginning of self-weight consolidation (2.29 kPa) is represented by
 264 an arrow and was calculated using the mean initial density (ρ_0) and the mean initial height, both presented in
 265 Table 2. This estimated value is quite close to the highest average EPWP at 0 m (~ 2.24 kPa shown in Fig. 4).
 266 At the very beginning of the test (1-minute reading), dissipation of EPWP was only observed at the bottom. As
 267 the test progressed, dissipation of EPWP moved from the initial triangular EPWP distribution, particularly near
 268 the bottom of the sample. As long as the self-weight consolidation had not reached a specific elevation,
 269 dissipation curves above this elevation were nearly parallel to the initial EPWP distribution curve. This typical
 270 pattern is associated with self-weight consolidation in settling columns with an impervious base, and shows that
 271 the process started from the bottom up (Sills 1997; Masutti 2001). For instance, the 600-minute profile shows

272 that the process of self-weight consolidation already reached 0.2 m because the profile comprised between 0.1
273 m and 0.2 m followed a steeper slope than the initial distribution.
274



275
276 **Fig. 4.** Evolution of average dissipation of excess pore water pressure with time and standard deviations for the
277 four tests performed in the 300-mm-high settling column
278



279
 280
 281
 282
 283
 284
 285
 286
 287
 288
 289
 290
 291

Fig. 5. Elevation versus average excess pore water pressure for the four tests performed in the 300-mm-high settling column

Self-weight and primary consolidation: Consolidometer and oedometer tests

Five tests were performed using the consolidometer to evaluate the $e - \sigma'_v$ relationship under a low effective stress range. Table 3 presents a summary of the main characteristics of samples C1 to C5. In the beginning of each test the samples had a similar height (H_0), therefore the same water pressure conditions. The initial void ratios (e_0) of the 5 experiments were approximately 1.3, while initial densities (ρ_0) were similar to those of the settling column experiments.

292 Fig. 6 presents the average void ratio versus vertical effective stress obtained in the consolidometer (lower stress
293 range) and in the oedometric apparatus (higher stress range). The load range of the consolidometer was
294 comprised between 0.06 kPa and 8.80 kPa. The results followed a rather similar trend for all tests, albeit a slight
295 scatter in void ratios, which nonetheless decreased with the increase in vertical effective stress. A similar trend
296 was obtained by Liu and Znidarcic (1991). As in the majority of soft soils such as TT, the $e - \sigma'_v$ relationship at
297 low effective stresses is greatly dependent on the initial void ratio and is not unique (Imai 1981; Been and Sills
298 1981; Liu and Znidarcic 1991). The consolidation behavior for loads greater than 8.80 kPa was obtained using
299 the oedometer cell. The primary consolidation in the consolidometer experiments started at initial void ratios
300 varying between 1.11 and 1.19, while the initial void ratios in the oedometer varied between 0.78 and 0.83.
301 Sample preparation, mainly compaction, induced stiffening of the material, thus lower void ratios. Hence, the
302 compression indexes (C_c) at lower effective stresses were higher than those determined using the oedometer.

303

304 Fig.6 shows more scattering in the results from the consolidometer than those from the oedometer tests and
305 there is one order of magnitude between the standard deviations obtained in the two types of tests. The slight
306 variation in C_c observed in the 5 tests performed in the consolidometer possibly relates to the accuracy of the
307 adopted experimental method. Moreover, the void ratio during self-weight consolidation was non-uniform over
308 the entire depth. As reported by Liu (1990), the use of an average value over the whole sample (as was the case
309 with the oedometer tests) can raise concerns. To overcome these limitations, other apparatus or methods might
310 be recommended to obtain the $e - \sigma'_v$ relationship at low effective stresses; i.e. the hydraulic consolidation test
311 (Imai 1979; Abu-Hejleh et al. 1996; Fox and Baxter 1997) or actual density measurements with non-destructive
312 readings using x-ray or γ -ray, during self-weight consolidation (Been and Sills 1981; Alexis et al. 2004;
313 Bartholomeeussen et al. 2002; Pedroni 2011; Masutti 2001; Tan et al. 1988).

314

315 Fig 7. shows that a compressibility relationship ($e - \sigma'_v$) for low vertical effective stresses was found from the
316 consolidometer results. The latter is comprised between the estimated vertical effective stress at a void ratio of
317 1.3 and the theoretical vertical effective stress reached in the 300-mm-high settling column. The $e - \sigma'_v$
318 relationship was estimated by means of a power law of the form $e = A\sigma'^B$. (Carrier III et al. 1983; McVay et al.
319 1986; Somogyi 1980; Huerta and Rodriguez 1992; Stone et al. 1994; Aydilek et al. 2000). The power law was
320 fitted by regression analysis using the average void ratio at each stress. This best-fit was used as a first attempt
321 to reproduce the self-weight consolidation behavior in a CS2 simulation.

322

323

324

325

326

327

328

329

330

331

332

Table 3. Summary of the five experiments in the consolidometer setup

Test	H_0 (m)	Initial void ratio, e_0	ρ_0 (kg/m ³)	Mass of tailings deposited (g)	H_f (m)	Vertical strain (%)	Height of supernatant water (m)	Dry solids mass (g)	Void ratio at 0.06 kPa
C1	0.094	1.28	1711.2	1295.63	0.085	9.7	0.009	862.40	1.13
C2	0.097	1.27	1702.7	1330.58	0.087	10.4	0.01	900.53	1.14
C3	0.096	1.30	1715.8	1326.85	0.087	9.4	0.009	899.94	1.13
C4	0.086	1.29	1704.4	1180.07	0.077	10.5	0.009	800.61	1.11
C5	0.085	1.30	1684.8	1152.85	0.078	8.3	0.01	782.72	1.20

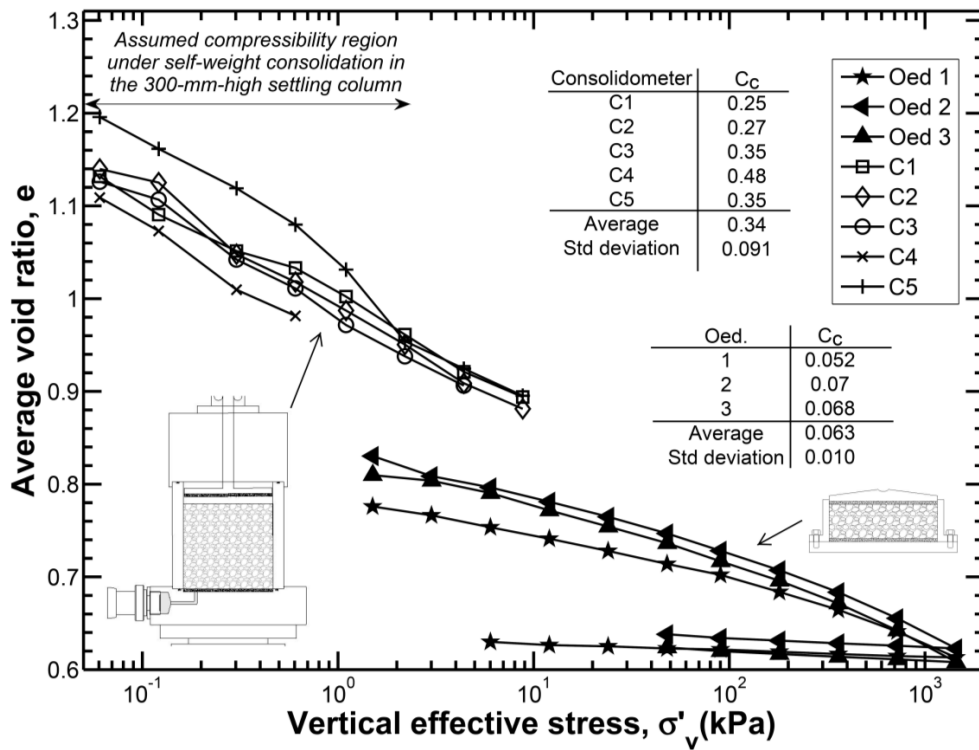
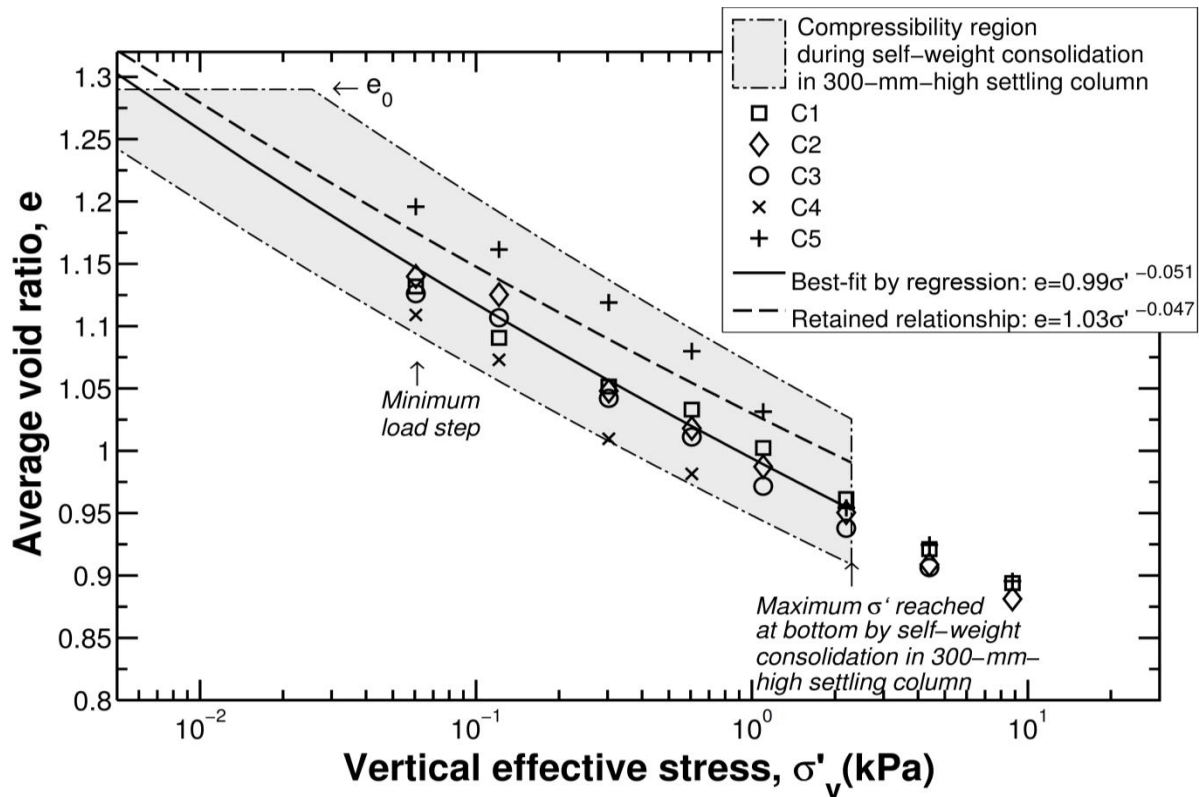


Fig. 6. Compressibility (average void ratio versus vertical effective stress) of experiments in consolidometer setup and oedometer cell



339
340 **Fig. 7.** Compressibility (average void ratio versus vertical effective stress) from the five experiments in the
341 consolidometer setup
342

343 **REPRODUCTION OF EXPERIMENTAL SELF-WEIGHT CONSOLIDATION**
344

345 In addition to the best-fit compressibility relationship obtained in Fig. 7, a hydraulic conductivity versus void ratio
346 relationship was obtained from falling head permeability tests performed in the oedometer cell. To prevent
347 seepage-induced consolidation in the oedometer cell, hydraulic conductivity measurements were not performed
348 at void ratios greater than $e=0.7$. Best-fit regression of the experimental results by means of a power law ($k =$
349 Ce^D) is generally reported to represent the k - e relationship for soft soils (Jeeravipoolvarn et al. 2009a; Pane and
350 Schiffman 1997; Gjerapic and Znidarcic 2007). Thus, the following hydraulic conductivity relationship was
351 estimated from a best-fit regression analysis: ($k(m/s) = 2.1 \times 10^{-7} e^{3.29}$).
352

353 Both best-fit relationships obtained by regression analysis ($e - \sigma'_v$ and $k - e$) were used in the first CS2
354 simulation (results not shown herein), which showed that in terms of mechanical response (total settlement and
355 final void ratio distribution), CS2 accurately reproduced the experimental results. However, the reproduction
356 overestimated the time of dissipation of EPWP. Subsequently, the constitutive parameters (A, B, C and D) were
357 optimized to determine the relationships giving the best reproduction of the experimental EPWP response, the
358 tailings-water interface settlement and the final void ratio distribution.
359

360 Suthaker and Scott (1994) and Bharat and Sharma (2011) noted that parameters A and B seem to have little
361 influence on the tailings-water interface response, but their influence on the final void ratio distribution is

362 important. On the other hand, parameter D considerably affects both the settlement response and final void ratio
363 distribution. Suthaker and Scott (1994) also reported that the change in the compressibility characteristics (A and
364 B) does not affect the short-term prediction of EPWP while the long-term prediction is slightly affected. They also
365 reported that the variation of parameter D has considerable effects on the EPWP response.

366

367 The parameters retained from this optimization process including the constitutive relationships are presented in
368 Table 4 and in Fig.7. Both constitutive relationships used 51 discrete data points. The self-weight consolidation
369 was modeled with a 0.3 m high sample subdivided in 50 vertical elements ($R_f=50$). An initial vertical effective
370 stress (q_o) of 0.0083 kPa and an initial hydraulic conductivity (k_{qo}) of 8.11×10^{-7} m/s were derived from the
371 retained constitutive relationships for the homogeneous initial void ratio of 1.29. The top boundary was
372 considered as drained while the bottom boundary was considered undrained. The water was maintained at a
373 constant elevation, which was equal to the initial height (0.3 m).

374

375 Fig.8 presents the evolution of EPWP with time at the three elevations corresponding to the positions of the
376 pressure transmitters. CS2 accurately reproduces the immediate startup of the EPWP dissipation at the bottom.
377 At 0.1 m and 0.2 m above bottom, CS2 quite accurately reproduces the pseudo-linear decrease in EPWP before
378 the start of the self-weight consolidation (change in slope). For instance, at 0.2 m, CS2 predicts the start of the
379 self-weight consolidation after approximately 540 min. The slope of the pseudo-linear portions of the
380 experimental curves is slightly steeper, which may be attributed to several factors: superficial sedimentation, non-
381 unique experimental compressibility relationship (Been and Sills 1981; Hawlader et al. 2008) or discrepancy
382 between constitutive relationships and the self-weight consolidation behavior. The end of self-weight
383 consolidation at 1440 min is also closely reproduced by CS2. Beside the pore water pressure response, Fig.8
384 also shows the mechanical response of CS2 at the end of the simulation. CS2 reproduces a void ratio of 1.15 at
385 the top of the column and 0.99 at the bottom while the tailings-water interfaces underwent a vertical strain of
386 11.0%. All those values are nearly the same as the experimental values from the 300-mm-high settling column.

387

388 The reproduction of the experimental results proved to be successful as confirmed by the evolution of the EPWP
389 with elevation (Fig.9). The theoretical experimental maximum EPWP is indicated by an arrow ($Max \mu_e =$
390 2.29 kPa). The EPWP profiles are calculated by CS2 using the density, pore water pressure conditions and
391 elevation at each element of the discretized geometry. The 1-minute profile determined by CS2 indicates that the
392 model had not begun to consolidate under its own weight at this time as the calculated EPWP is 2.24 kPa at 0 m
393 (the experimental value was 2.21 kPa) and the EPWP profile was linear throughout the column. The reproduced
394 intercept with the y-axis after 1 min is 0.3 m, which was the average initial height of the samples. From 50
395 minutes on, the curved ends of the EPWP profiles indicated the portion of the column that had begun to
396 consolidate under its own weight. Based on the profiles determined by CS2, self-weight consolidation had been
397 initiated for a height of approximately 0.06 m at 100 min and after 300 min, it had reached 0.12 m above the
398 bottom. Moreover, the intercept with the y-axis went down as the tailings-water interface settled due to self-
399 weight consolidation at lower depths. It is also worth noting that CS2 has the capacity to reflect the fact that
400 dissipation of EPWP by self-weight consolidation at the bottom affects the EPWP at the top as observed by
401 experimental results.

402

403

Table 4. Input parameters used in CS2

Initial height (m)	Initial void ratio	Initial effective stress, q_0 (kPa)	K_{q_0} (m/s)	G_s	Constitutive relationships		Number of elements, R_j
					Compressibility $e = A\sigma'^B$	Hydraulic conductivity $k = Ce^D$	
0.3	1.29	0.0083	8.11×10^{-7}	2.76	A(kPa)= 1.03 B(-)= -0.047	C(m/s)= 3.5×10^{-7} D(-)=3.3	50

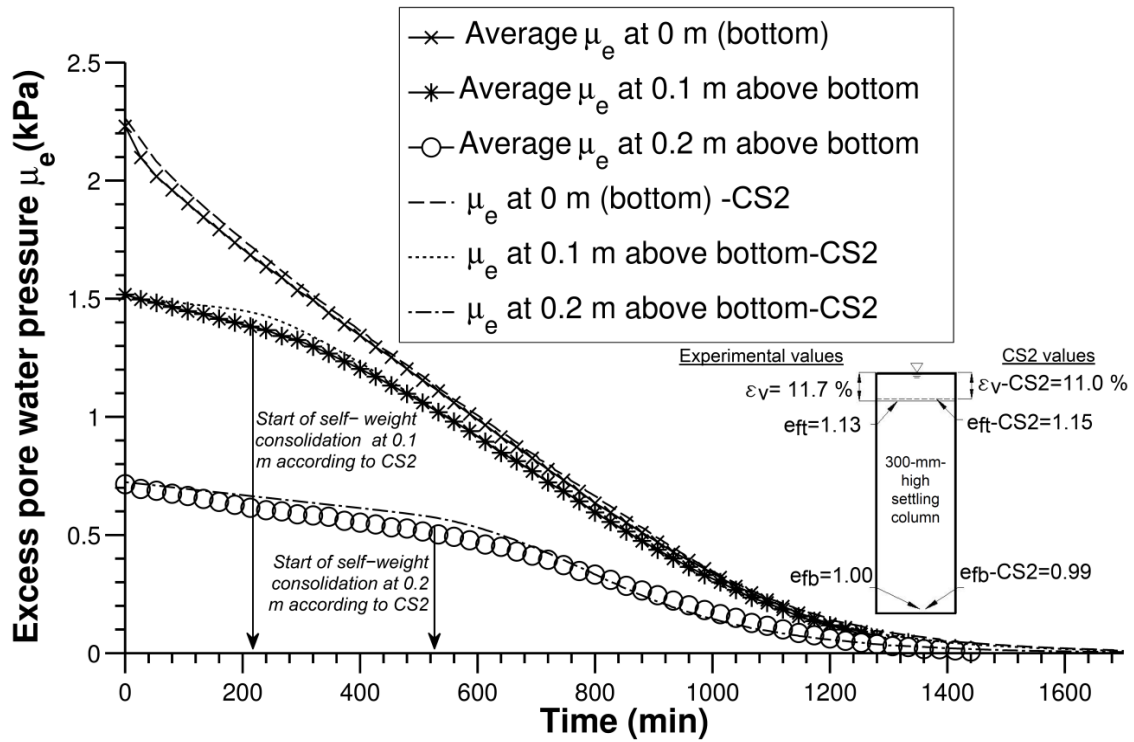
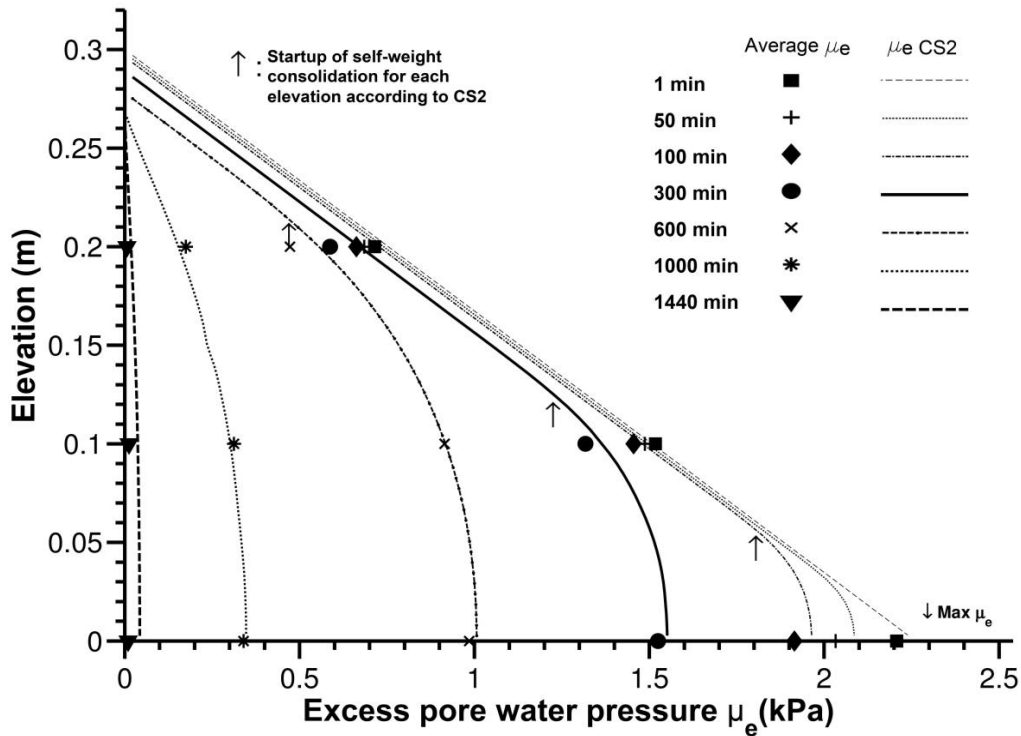


Fig. 8. Evolution of average dissipation of EPWP with time in the 300-mm-high column: experimental results and values reproduced by CS2



411
 412 **Fig. 9.** Profile of elevation versus EPWP in the 300-mm-high settling column: experimental results and values
 413 reproduced by CS2
 414

415 **Discussion**

416
 417 In the context of this study, a TT sample deposited to 68% of solids would undergo mainly self-weight
 418 consolidation. This initial void ratio is well below the critical void ratios reported by de Oliveira-Filho and van Zyl
 419 (2006), Bartholomeeusen et al. (2002) for silty materials. The sedimentation phase seems to be inhibited by the
 420 proximity of solid particles that can rapidly transmit their own weight to a soil structure supported at the bottom of
 421 the column and dissipate EPWP. The main EPWP decrease occurs by self-weight consolidation from the bottom
 422 and proceeds upward while a minor EPWP diminution is observed in the uppermost part of the column. The CS2
 423 simulations support that this minor dissipation seems to result mainly from settlement of the slurry height caused
 424 by self-weight consolidation and not because of potential sedimentation.
 425

426 CS2 proved quite capable of reproducing the behavior of thickened tailings under self-weight consolidation, be it
 427 the EPWP dissipation, the final settlement or the final void ratio distribution. This tends to confirm that the sole
 428 mechanism (or the main one) influencing settlement of TT initially deposited at 68% solids is probably self-weight
 429 consolidation. It is believed that CS2 would not have adequately reproduced the experimental behavior of the
 430 same material deposited at an initial void ratio higher than its critical void ratio. In fact, the prediction of the
 431 sedimentation combined with self-weight consolidation should lead to different profiles of EPWP as shown by
 432 Concha and Bürger (1998). Li and Williams (1995b), Sills (1998) and Masutti (2001) presented such
 433 experimental EPWP profiles of soils deposited below their structural density.
 434

435 The reproduction of the self-weight consolidation behavior in the 300-mm-high settling column proved to be
436 reliable in using the one-dimensional model CS2 and the retained constitutive relationships. The transposition of
437 this model to a larger scale should be conducted with caution given the nature of the constitutive relationships,
438 which might not represent the behavior at higher effective stresses (Carrier III et al. 1983) and the one-
439 dimensional formulation.

440

441

442 **CONCLUSION**

443

444 A 300-mm-high settling column was used to assess the self-weight consolidation behavior of TT. An accurate
445 monitoring of total pore water pressure showed that self-weight consolidation finishes after 24 hours at 68%
446 solids and confirmed that the mechanism moves from the bottom up. A consolidometer was used to establish an
447 initial estimate of the $e - \sigma'_v$ relationship at low effective stresses. The CS2 numerical model was used to
448 calibrate the $e - \sigma'_v$ and the $k - e$ relationships in order to reproduce the self-weight consolidation from the 300-
449 mm-high settling column. Slight differences were observed between the calibrated and the experimental best-fit
450 relationships.

451

452 Analysis carried out with CS2 by using calibrated constitutive relationships highlighted the capabilities of this
453 model to accurately reproduce the self-weight consolidation of TT be it the dissipation of EPWP or the
454 mechanical response. Moreover, the experimental study coupled with the numerical reproduction have confirmed
455 that sedimentation can be neglected when tailings are thickened to 68% solids. CS2 confirms the characteristics
456 of a typical profile of EPWP dissipation when self-weight consolidation is the sole mechanism at the very moment
457 of the deposition.

458

459 Identifying the main mechanisms behind the settlement of TT is an advance for the mining industry as it enlarges
460 the knowledge related to TT. A better understanding of self-weight consolidation helps to identify processes
461 involved in TT settlement. This information is relevant to estimate the storage capacity of TDA, to evaluate the
462 freeboard of confining structures and to analyze the density distribution throughout the tailings deposit.

463

464

465 **ACKNOWLEDGEMENTS**

466 The authors would like to thank geotechnical technicians Jean-Guy Lemelin and Valérie Dumoulin for their
467 technical support. Funding for this research has been provided by the National Sciences and Engineering
468 Research Council (NSERC), the Fond Québécois pour la Recherche Nature et Technologies (FQRNT) and
469 Golder Associés Ltée. through a BMP-Innovation Scholarship.

470

471

472

473

474

475

REFERENCES

- Abu-Hejleh, A., Znidarčić, D., and Barnes, B. (1996). "Consolidation Characteristics of Phosphatic Clays." *J. Geotech. Eng.*, 122(4), 295-301.
- Alexis, A., Le bras, G., and Thomas, P. (2004). "Experimental bench for study of settling-consolidation soil formation." *Geotech Test J*, 27(6), 557-567.
- Aubertin, M., Bussière, B., and P. Chapuis, R. (1996). "Hydraulic conductivity of homogenized tailings from hard rock mines." *Canadian Geotechnical Journal*, 33(3), 470-482.
- Aydilek, A. H., Edil, T. B., and Fox, P. J. (2000). "Consolidation characteristics of wastewater sludge." *Geotechnics of High Water Content Materials*, January 28, 1999 - January 29, ASTM, Memphis, TN, USA, 309-323.
- Azam, S. (2011). "Large strain settling behavior of polymer-amended laterite slurries." *International Journal of Geomechanics*, 11(2), 105-112.
- Barbour, S. L., Wilson, G. W., Salvas, R. J., St Arnaud, L., and Bordin, D. (1993). "Aspects of environmental protection provided by thickened tailings disposal." *Proceedings of the International Congress on Mine Design*, A.A. Balkema, Kingston, Ont, Canada, 725-725.
- Bartholomeeusen, G., Sills, G. C., Znidarcic, D., Van Kesteren, W., Merckelbach, L. M., Pyke, R., Carrier, W. D., Lin, H., Penumadu, D., Winterwerp, H., Masala, S., and Chan, D. (2002). "Sidere: Numerical prediction of large-strain consolidation." *Geotechnique*, 52(9), 639-648.
- Been, k., and Sills, G. C. (1981). "Self-weight consolidation of soft soils: an experimental and theoretical study." *Géotechnique*, 31(4), 519-535.
- Berilgen, S. A., Berilgen, M. M., Ozaydin, K. I., and Bicer, P. (2006). "Assessment of consolidation behavior of golden horn marine dredged material." *Marine Georesources and Geotechnology*, 24(1), 1-16.
- Bharat, T. V., and Sharma, J. (2011). "Prediction of compression and permeability characteristics of mine tailings using natural computation and large-strain consolidation framework." *Geo-Frontiers 2011: Advances in Geotechnical Engineering, March 13, 2011 - March 16*, American Society of Civil Engineers (ASCE), Dallas, TX, United states, 3868-3877.
- Blight, G. E., and Steffen, O. K. H. (1979). "Geotechnics of gold mining waste disposal." *Proceedings of Current Geotechnical Practice in Mine Waste Disposal*, American Society of Civil Engineering, New York, 1-52.
- Bromwell, L. G., and Carrier, W. D. (1979). "Consolidation of fine-grained mining wastes." *Proceedings of the sixth Pan-American conference on soil mechanics and foundation engineering*, Lima, Peru, 293-304.
- Burger, R., and Concha, F. (1998). "Mathematical model and numerical simulation of the settling of flocculated suspensions." *Int. J. Multiphase Flow*, 24(6), 1005-23.
- Bussière, B. (2007). "Colloquium 2004: Hydrogeotechnical properties of hard rock tailings from metal mines and emerging geoenvironmental disposal approaches." *Canadian Geotechnical Journal*, 44(9), 1019-1052.
- Carrier III, W. D., Bromwell, L. G., and Somogyi, F. (1983). "Design capacity of slurried mineral waste ponds." *J. Geotech. Eng.*, 109(5), 699-716.

- Crowder, J. J. (2004). "Deposition, consolidation, and strength of a non-plastic tailings paste for surface disposal". Ph.D. University of Toronto (Canada), Canada.
- de Oliveira-Filho, W. L., and van Zyl, D. (2006). "Modeling discharge of interstitial water from tailings following deposition. Part 2: Application." *Solos e Rochas*, 29(2), 211-221.
- Demers Bonin, M., Nuth, M., Cabral, A., and Dagenais, A. -M. (2013). "Self-weight consolidation behavior of thickened gold tailings." *GeoMontreal 2013*, Montréal, 1-7.
- Elder, D. M. (1985). "Stress-Strain and strength behaviour of very soft soil sediment". DPhil thesis. University of Oxford, UK.
- Fahey, M., Helinski, M., and Fourie, A. (2010). "Consolidation in accreting sediments: Gibson's solution applied to backfilling of mine stopes." *Geotechnique*, 60(11), 877-882.
- Fourie, A. (2012). "Paste and thickened tailings: has the promise been fulfilled?" 4126-4135.
- Fox, P. J., and Baxter, C. D. P. (1997). "Consolidation properties of soil slurries from hydraulic consolidation test." *J.Geotech.Geoenviron.Eng.*, 123(8), 770-776.
- Fox, P. J., and Berles, J. D. (1997). "CS2: a piecewise-linear model for large strain consolidation." *Int.J.Numer.Anal.Methods Geomech.*, 21(7), 453-475.
- Fox, P. J. (2000). "CS4: A large strain consolidation model for accreting soil layers." *Geotechnics of High Water Content Materials, January 28, 1999 - January 29, ASTM*, Memphis, TN, USA, 29-47.
- Gibson, R. E., England, G. L., and Hussey, M. J. L. (1967). "Theory of one-dimensional consolidation of saturated clays -- 1." *Geotechnique*, 17(3), 261-273.
- Gjerapic, G., and Znidarcic, D. (2007). "A mass-conservative numerical solution for finite-strain consolidation during continuous soil deposition." *Geotech Spec Publ*, (157).
- Hawladar, B. C., Muhunthan, B., and Imai, G. (2008). "State-dependent constitutive model and numerical solution of self-weight consolidation." *Geotechnique*, 58(2), 133-141.
- Huerta, A., and Rodriguez, A. (1992). "Numerical analysis of non-linear large-strain consolidation and filling." *Computers and Structures*, 44(1-2), 357-365.
- Imai, G. (1981). "Experimental studies on sedimentation mechanism and sediment formation of clay materials." *Soils and Foundations*, 21(1), 7-20.
- Imai, G. (1980). "Settling behaviour of clay suspension." *Soils and Foundations*, 20(2), 61-77.
- Imai, G. (1979). "Development of a new consolidation test procedure using seepage force." *Soils and Foundations*, 19(3), 45-60.
- Jeeravipoolvarn, S., Chalaturnyk, R. J., and Scott, J. D. (2009a). "Sedimentation-consolidation modeling with an interaction coefficient." *Comput.Geotech.*, 36(5), 751-61.
- Jeeravipoolvarn, S., Scott, J. D., and Chalaturnyk, R. J. (2009b). "10 m standpipe tests on oil sands tailings: Longterm experimental results and prediction." *Canadian Geotechnical Journal*, 46(8), 875-888.
- Li, H., and Williams, D. J. (1995a). "Numerical modelling of combined sedimentation and self-weight consolidation of an accreting coal mine tailings slurry." *Part 1 (of 2)*, Hiroshima, Japan, 441-446.
- Li, H., and Williams, D. J. (1995b). "Sedimentation and self-weight consolidation behaviour of coal mine tailings." *Part 1 (of 2)*, Hiroshima, Japan, 117-122.

- Liu, J. (1990). "Determination of soft soil characteristics". Ph.D. University of Colorado at Boulder, United States -- Colorado.
- Liu, J., and Znidarcic, D. (1991). "Modeling one-dimensional compression characteristics of soils." *J.Geotech.Eng.*, 117(1), 162-169.
- Masutti, F. (2001). "Étude expérimentale de la sédimentation-consolidation et de l'acquisition de résistance d'un sol fin". Thèse de Doctorat. École Nationale Supérieure de Géologie de Nancy, Institut National Polytechnique de Lorraine, France.
- McPhail, G., Noble, A., Papageorgiou, G., and Wilkinson, D. (2004). "Development and implementation of thickened tailings discharge at Osborne Mine, Queensland, Australia." *2004 International Seminar on Paste and Thickened Tailings*, 1-32.
- McVay, M., Townsend, F., and Bloomquist, D. (1986). "Quiescent consolidation of phosphatic waste clays." *J.Geotech.Eng.*, 112(11), 1033-1049.
- Migniot, C. (1989). "Tassement et rhéologie des vases Première partie." *La Houille Blanche*, (1), 11-30.
- Mikasa, M. (1965). "Consolidation of soft clay -- New consolidation theory and its application." *Civil Engineering in Japan*, 4 21-26.
- Mittal, H. K., and Morgenstern, N. R. (1976). "Seepage control in tailings dams." *Canadian Geotechnical Journal*, 13(3), 277-293.
- Morris, P. (2002). "Analytical Solutions of Linear Finite-Strain One-Dimensional Consolidation." *J.Geotech.Geoenviron.Eng.*, 128(4), 319-326.
- Oxenford, J., and Lord, E. R. (2006). "Canadian experience in the application of paste and thickened tailings for surface disposal." *Paste 2006*, Australian Centre for Geomechanics, Limerick, Ireland, 93-105.
- Pane, V., and Schiffman. (1997). "The permeability of clay suspensions." *Geotechnique*, 47(2), 273-288.
- Pane, V., and Schiffman, R. L. (1985). "Note on sedimentation and consolidation." *Geotechnique*, 35(1), 69-72.
- Pedroni, L. (2011). "Étude expérimentale et numérique de la sédimentation et de la consolidation des boues de traitement des eaux acides". Ph.D. École Polytechnique, Montreal (Canada), Canada.
- Robinsky, E. I. (1999). *Thickened tailings disposal in the mining industry* Quebecor Printpak, Toronto.
- Robinsky, E. I. (1975). "Thickened discharge-A new approach to tailings disposal." *CIM Bulletin*, 68(764), 47-53.
- Schiffman, R. L., Vick, S. G., and Gibson, R. E. (1988). "Behavior and properties of hydraulic fills." *Geotechnical Special Publication*, 166-202.
- Sills, G. (1998). "Development of structure in sedimenting soils." *Philosophical Transactions of the Royal Society A: Mathematical, Physical and Engineering Sciences*, 356(1747), 2515-2534.
- Sills, G. C. (1997). "Consolidation of cohesive sediments in settling columns." *Cohesive Sediments*, John Wiley & Sons Ltd., 107-120.
- Somogyi, F. (1980). "LARGE-STRAIN CONSOLIDATION OF FINE-GRAINED SLURRIES." *Ann.Biomed.Eng.*, 1-16.
- Stone, K. J. L., Randolph, M. F., Toh, S., and Sales, A. A. (1994). "Evaluation of consolidation behavior of mine tailings." *J.Geotech.Eng.*, 120(3), 473-490.

- Suthaker, N. N., and Scott, J. D. (1994). "Large strain consolidation of oil sand fine tails in a wet landscape." *47th Canadian Geotechnical Conference*, Halifax, 514-523.
- Tan, S., Tan, T., Ting, L. C., Yong, K., Karunaratne, G.-P., and Lee, S. (1988). "Determination of consolidation properties for very soft clay." *Geotech Test J*, 11(4), 233-240.
- Tan, T.-S., (1995). "Sedimentation to consolidation: A geotechnical perspective." *Part 2 (of 2)*, Hiroshima, Japan, 937-937.
- Tan, T. S., Yong, K. Y., Leong, E. C., and Lee, S. L. (1990). "Sedimentation of clayey slurry." *J.Geotech.Eng.*, 116(6), 885-898.
- Toorman, E. A. (1999). "Sedimentation and self-weight consolidation: Constitutive equations and numerical modelling." *Geotechnique*, 49(6), 709-726.
- Townsend, F. C., and McVay, M. C. (1990). "SOA. Large strain consolidation predictions." *J.Geotech.Eng.*, 116(2), 222-243.
- Williams, M. P. A., and Ennis, P. C. (1996). "Suitability of the central thickened discharge method for nickel tailings disposal in Western Australia." *Proceedings of the 1996 Nickel Conference, November 27, 1996 - November 29*, Australian Inst of Mining & Metallurgy, Kalgoorlie, Aust, 275-283.
- Wong, R. K., Mills, B. N., and Liu, Y. B. (2008). "Mechanistic model for one-dimensional consolidation: Behavior of nonsegregating oil sands tailings." *J.Geotech.Geoenviron.Eng.*, 134(2), 195-202.
- Xie, K. H., and Leo, C. J. (2004). "Analytical solutions of one-dimensional large strain consolidation of saturated and homogeneous clays." *Comput.Geotech.*, 31(4), 301-314.
- Yunxin (Jason), Q., and Segoo, D. C. (2001). "Laboratory properties of mine tailings." *Canadian Geotechnical Journal*, 38(1), 183-190.